Acta Crystallographica Section D
Biological Crystallography
ISSN 0907-4449

Assessment of a preliminary solubility screen to improve crystallization trials: uncoupling crystal condition searches

Aude Izaac,[a] Constance A. Schall[b] and Timothy C. Mueser[a]*

[a]Department of Chemistry, The University of Toledo, Toledo, OH 43606, USA, and [b]Department of Chemical Engineering, The University of Toledo, Toledo, OH 43606, USA

Correspondence e-mail: timothy.mueser@utoledo.edu

Received 24 January 2006
Accepted 17 May 2006

The utility of a preliminary solubility screen has been assessed on ten test proteins. It is proposed that maximizing the protein solubility prior to crystal setups is likely to improve crystal growth. In crystallization setups, drops of a protein solution are mixed with various crystallization solutions which are then allowed to equilibrate. The protein solutions usually contain a salt and buffer which are present as a constant in all crystal screens. The propensity for crystallization, driven by three components of sparse-matrix screens, the buffers, salts and precipitating agents, could potentially be masked by the components of the protein solution. Ten test proteins were dissolved in a standard buffer (100 m*M* NaCl, 50 m*M* Tris–HCl pH 7.5) and in customized optimal buffers determined to maximize solubility. The proteins were then subjected to the Index (Hampton Research) 96-well sparse-matrix crystal screen and to a precipitant/precipitant–additive screen described here. Five of the ten proteins studied showed twofold to fourfold increases in the saturation level from standard to optimal buffer, two showed slight improvement and three showed a slight decrease. Microcrystals were obtained for all proteins and optimal buffer increased the appearance of crystals for eight of the ten proteins.

1. Introduction

The crystallization of macromolecules involves multi-parametric experiments of an enormous number of physical and chemical parameters. The high-profile nature of protein structure determination has driven the field towards high-throughput robotic techniques to enable the investigation of these vast quantities of conditions (Cumbaa *et al.*, 2003; Rupp *et al.*, 2002; Page *et al.*, 2003). The primary approach utilized by most investigators is to prepare or purchase a collection of public domain or commercially available sparse-matrix crystal screens and subject the proteins of interest to these screens at a few selected temperatures. Analysis of crystallization results then leads to further trials until crystal optimization has been achieved.

The sparse-matrix screens are Monte Carlo methods for randomly testing the chemical space of crystallization. The first sparse-matrix screen introduced (Jancarik & Kim, 1991) was based on positive results derived from the NIST/CARB Biological Macromolecule Crystallization Database (Gilliland *et al.*, 1994). Crystal Screen 1, as it is now known, is a set of known positive conditions; it is not truly a random approach but it has become an essential first attempt for crystallization. A multitude of additional screens have been developed, some based on a random approach (Cudney *et al.*, 1994) and others

based on systematic analysis (Brzozowski & Walton, 2001; McPherson, 2001; Gao *et al.*, 2005). Strategies for crystallization and optimization are useful in guiding our research (McPherson, 1999; D'Arcy, 1994). Approaches have been devised for the analysis of crystal screen results from the incomplete factorial approach (Carter & Carter, 1979) to sophisticated neural networks (DeLucas *et al.*, 2003). However, positive results are required to drive the next stages of experimentation. In the absence of positive hits, one can mine the results for less than obvious positive conditions and redefine the search (Page & Stevens, 2004).

Improvements in the preparation of macromolecules for crystal screening have also been a fruitful avenue of research. The use of dynamic light scattering has been very important in preparation of homogeneous samples for crystallization trials (Bonneté & Vivarès, 2002). Studies of nucleation have provided valuable insight into the stages of crystal development (Durbin & Feher, 1996; Tardieu *et al.*, 2002). The quest for soluble and homogeneous samples has been an essential component of crystallization research. Obviously, if the protein is not soluble then crystals will not have material for formation. The Optimum Solubility (OS) screening method has been presented (Jancarik *et al.*, 2004) which combines vapour diffusion and dynamic light-scattering measurements with buffer and additive screens to define monodisperse samples and assess potential precipitating agents. Earlier, the Reverse Screen was proposed in which precipitating agents and varying protein concentrations were used to construct phase diagrams (Stura *et al.*, 1994). This screen suggests strategies to confine the search parameters for crystallization trials and define novel systematic searches for each macromolecule studied. Most recently, a method for assessing crystal screen results for protein solubility has been described (Collins *et al.*, 2005).

Recently, we presented a simple solubility screen for improving crystallization trials (Collins *et al.*, 2004). The solubility screen was derived from the 'Ion Screen', a systematic crystallization screen (Mueser *et al.*, 2000) that is the precursor to Hampton Research's 'PEG/Ion screen' (Bob Cudney, personal communication). We obtained diffraction-quality crystals of an archaeal nuclease where previous attempts without optimization yielded no useful information. In that article, we proposed that in enhancing solubility the path to crystal formation is favored and the path to amorphous phase formation is suppressed. This hypothesis is supported by an analysis of the energetics of aggregate formation (Durbin & Feher, 1996). The free-energy change upon addition of a molecule to an amorphous aggregate is independent of aggregate size, where in crystallization the free-energy change exhibits a maximum with respect to aggregate size. In other words, the energy barrier to aggregate formation is near zero for amorphous aggregates and is higher for crystal formation. Crystallization is preceded by a lag time needed to form aggregates of suitable size to overcome this energy barrier. For precipitation (amorphous phase formation), kinetics of aggregate formation is rapid. Precipitation can dominate for kinetic reasons when the energy barrier to crystallization is very high, leading to excessive lag times compared with amorphous precipitation (Durbin & Feher, 1996).

Solubility provides an indirect measure of the energetics of crystal nucleation kinetics. In nucleation induction-time studies of lysozyme crystals (Kulkarni & Zukoski, 2002), solubility enhancement was correlated with a decrease in the crystal–liquid surface tension. In classical nucleation theory, a decrease in surface tension lowers the energetic barrier to nucleation through an exponential function. As a corollary to this, it is expected that as solubility increases, crystal nucleation will occur at lower supersaturation owing to the reduced energetic barrier. Therefore, improvement of solubility will allow subsequent crystal growth at lower supersaturation and perhaps more uniform crystal growth. If solubility enhancement is too pronounced, formation of amorphous solid will be favored. Optimizing solubility is, in essence, balancing the energetics of solid formation to lower the barrier to crystal formation to kinetically favour crystallization over precipitation while avoiding near-elimination of the energy barrier which favors precipitation.

With this in mind, we investigated the utility of a solubility screen on well known 'test' proteins to determine if improvements are possible and can be determined easily. We have also attempted to uncouple the three major constituents of crystallization screens: salts, buffers and precipitating agents. Although salts can also serve as precipitants, low concentrations of salts are often required to stabilize or salt proteins into solution (Collins, 2004). Here, we propose that the salt and buffer components can be defined by a solubility screen and precipitating agents and additives can then be assessed using vapor-diffusion crystallization experiments. Two precipitant screens were tested: a commercial screen and a precipitant/precipitant–additive screen, P/PA, designed for this study. The P/PA screen was designed in an attempt to uncouple selection of the buffer and salt from that of precipitant/additive.

2. Experimental

Ten test proteins were selected from the lists used in comparative studies of crystal screening methods (Cudney *et al.*, 1994; Wooh *et al.*, 2003). The proteins, chosen based on availability and known crystallizability, were purchased as lyophilized powders or as concentrated solutions from Sigma [catalyse (C40), subtilisn (P5380), thaumatin (T7638), α-lactalbumin (L5385), trypsin (T1426), pepsin (P7012), ovalbumin (A5503) and myoglobin (M0630)] and from Hampton Research [xylanase (HR7-106) and D-xylose isomerase (HR7-102)]. These proteins were first subjected to a solubility screen. The results were then used to create an optimized solution for each protein and saturation levels determined for each solution and for the protein in a standard solution. The proteins in standard and in optimized buffer solutions were subjected to a commercial sparse-matrix crystal screen and to a new precipitant/precipitant–additive screen (P/PA) described here.

Table 1
Relative solubility results.

Solubility-screen results are presented for recovery from precipitation by 20%(*w*/*v*) PEG 8000 using 100 m*M* buffers or salts. The anionic salts with buffering capacity were adjusted to pH 7.0 with NaOH prior to use. Common counterions allow cross-mixing of ions to establish the saturation level. The results for catalase (Cat), subtilisin (Sub), thaumatin (Tha), xylanase (Xyl), α-lactalbumin (Lac), D-xylose isomerase (XI), trypsin (Try), pepsin (Pep), ovalbumin (Ova) and myoglobin (Myo) in A_{595} absorbances from the Coomassie protein dye assay are shown (nd indicates not detected). No attempt was made to relate the assay to actual concentration, as relative values are needed for this assessment. For catalase, sodium citrate and Na TAPS buffer solutions show distinct increases in solubility compared with water, while most other salts and buffers decrease solubility. All proteins display some residual solubility in water alone after PEG precipitation, especially thaumatin and xylanase, where the salts and buffers decreased solubility. These initial solubility profiles were then used to select an optimal salt and buffer combination for use in crystal screens.

	Cat	Sub	Tha	Xyl	Lac	XI	Try	Pep	Ova	Myo
H_2O	0.04	0.25	0.48	0.32	0.06	0.01	0.18	0.02	0.40	0.04
Cation screen										
NH_4Cl	nd	0.20	0.17	0.16	0.21	0.04	0.11	0.02	0.03	nd
NaCl	0.02	0.22	0.15	0.17	0.18	0.03	0.12	nd	0.01	nd
KCl	nd	0.22	0.16	0.13	0.21	0.02	0.12	nd	0.02	nd
LiCl	0.01	0.26	0.18	0.19	0.08	0.02	0.10	nd	0.13	0.03
$MgCl_2$	0.02	0.22	0.17	0.12	0.30	nd	0.11	nd	0.08	0.02
$CaCl_2$	0.04	0.40	0.16	0.22	0.29	0.08	0.10	nd	0.06	0.01
Anion screen										
Sodium formate	0.01	0.25	0.16	0.25	0.09	0.12	0.11	nd	0.15	0.01
Sodium acetate	nd	0.27	0.16	0.12	0.16	0.31	0.10	nd	0.15	0.03
Sodium cacodylate	0.02	0.24	0.13	0.17	0.26	0.39	0.13	nd	0.32	0.07
Sodium sulfate	nd	0.23	0.19	0.24	0.11	0.02	0.03	nd	0.09	nd
Sodium phosphate	0.14	0.23	0.24	0.17	0.27	0.30	0.05	nd	0.53	0.04
Sodium citrate	0.35	0.15	0.20	0.22	0.51	0.26	0.15	nd	0.36	0.07
Good buffers										
Na MES pH 5.6	0.01	0.26	0.37	0.29	0.12	0.18	0.09	nd	0.25	0.09
Na PIPES pH 6.5	nd	0.27	0.47	0.23	0.16	0.21	0.09	nd	0.32	0.08
Na HEPES pH 7.5	0.08	0.27	0.36	0.23	0.28	0.21	0.09	nd	0.91	0.05
Na TAPS pH 8.5	0.29	0.32	0.28	0.31	0.38	0.40	0.11	0.63	0.92	0.64

2.1. Preparation of proteins

Solutions of proteins obtained in powder form were prepared by layering 10 mg powder on 200 µl distilled water and allowing the powder to slowly dissolve overnight at ambient temperature (295 ± 1 K). The solutions were then filtered using centrifugal filter units (Amicon, 0.45 µm Durapore Ultra-MC, 0.5 ml capacity). The proteins obtained as solutions (xylanase and D-xylose isomerase; Hampton Research) were dialyzed against distilled water overnight using dialysis cassettes (Pierce, 10 000 Da molecular-weight cutoff, 0.1–0.5 ml Slide-A-Lyzer) and filtered as described above. A few proteins required additional steps in preparation. The protease inhibitor AEBSF–HCl (CalBiochem) was added to the serine proteases to prevent degradation. Myoglobin was obtained in the dark brown aquomet form. After dissolution in water, a few crystals of sodium azide were added and the bright red solution was then filtered through a Sephadex G25 column, pooling the main red fraction.

2.2. Solubility screen

Most proteins dissolved or dialysed in distilled water will precipitate. The proteins chosen for this study were all soluble in water to a large extent and a precipitating agent was required to partition the samples between solid and liquid phases. Anionic and cationic series of salts with common counterions and a set of Good buffers (Good *et al.*, 1966) ranging from pH 5.6 to 8.5 were used in this study (Table 1). For each sample, 150 µl filtered protein was forced to precipitate by the addition of 190 µl 40%(*w*/*v*) PEG 8000 [ambient temperature (295 ± 1 K), 15 min]. The suspension was mixed with a pipette and 18 µl aliquots were added to 17 small centrifuge tubes (Eppendorf, 1.5 ml capacity). To each aliquot, 2 µl of the corresponding 1 *M* salt or buffer solution was added, mixed by agitation to resuspend the precipitated protein and allowed to stand [ambient temperature (295 ± 1 K), 20 min]. At this point, the concentrations in each 20 µl sample were 20%(*w*/*v*) PEG 8000 and 100 m*M* salt or buffer. The solutions were centrifuged [20 000*g*, 4 min, ambient temperature (295 ± 1 K)] and the supernatant of each tube was tested for soluble protein using a BioRad Protein Assay (5 µl protein, 995 µl 1× BioRad reagent). The samples were incubated for 5 min and absorbance was measured at 595 nm using a UV–Vis spectrophotometer (Agilent 8453) and disposable semi-microcuvettes. Relative measures of solubility were required for this initial step. Accurate measures of protein concentration were completed for the final solutions as described below.

2.3. Optimized solutions and saturation determination

The salt and buffer giving the highest solubility values for each protein comprise the optimized conditions for that protein. Two new solutions were prepared for each protein as described above, one in a standard chromatography buffer (50 m*M* Tris–HCl pH 7.5, 100 m*M* NaCl) and a second in the optimized buffer (100 m*M* salt, 50 m*M* buffer). The saturation level of each protein was then measured in both solutions by concentrating small samples in centrifugal concentrators (Amicon, Microcon YM-10, 10 000 Da molecular-weight

Table 2
Test proteins used and solubility optimization results.

Ten test proteins were subjected to the solubility screen. The saturation level was determined using centrifugal concentrators and values are reported for proteins in standard buffer (100 m*M* NaCl, 50 m*M* Tris–HCl pH 7.5) and for the customized optimal buffers. The proteins are listed according to improvements in solubility, with the ratio of saturated concentrations optimal to standard buffers reported in the final column. Also provided are the calculated pIs (*ProtParam*; Gasteiger *et al.*, 2003) and sources of the proteins. The first five proteins display significant improvement in solubility, the next two display modest improvement and the final three show a decrease in solubility.

	Protein (source, calculated pI)	Optimal buffer (50 m*M*) and salt (100 m*M*)	Solubility in standard buffer (mg ml^{-1})	Solubility in optimized buffer (mg ml^{-1})	Ratio (optimized/ standard)
1	Catalase (bovine, 6.4)	Na TAPS pH 8.5, trisodium citrate	11	40	3.64
2	Subtilisin Carlsberg (*Bacillus licheniformis*, 6.6)	Na TAPS pH 8.5, 10 m*M* $CaCl_2$	17	52	3.06
3	Thaumatin (*Thaumatococcus danellii*, 8.5)	Na PIPES pH 6.5, no salt	17	50	2.94
4	Xylanase (*Tricoderma longribrahiatum*, 9.0)	Na TAPS pH 8.5, sodium formate	28	76	2.71
5	α-Lactalbumin (bovine, 4.8)	Na TAPS pH 8.5, trisodium citrate	22	41	1.86
6	D-Xylose isomerase (*Streptomyces rubiginosus*, 5.0)	Na TAPS pH 8.5, sodium cacodylate pH 7.0	144	178	1.24
7	Trypsin (bovine, 8.7)	Na TAPS pH 8.5, no salt	46	50	1.09
8	Pepsin (porcine, 3.4)	Na TAPS pH 8.5, no salt	66	58	0.88
9	Ovalbumin (chicken, 5.2)	Na HEPES pH 7.5, no salt	148	120	0.81
10	Myoglobin (equine, 7.4)	Na TAPS pH 8.5, no salt	122	86	0.71

cutoff; 0.5 ml capacity, 10 000*g*). The supernatant was sampled every 10 min until precipitation was noticed or the concentration levelled off. For accuracy, the samples were mixed and briefly centrifuged before a final concentration was measured. To obtain a better estimate of protein concentration, the ExPasy Swiss Protein Database *ProtParam* tool was used to calculate an absorbance conversion factor and isoelectric points based on amino-acid content (Gasteiger *et al.*, 2003). The conversion factors of $A_{280}^{0.1\%}$ (1 mg ml^{-1}) are 1.037 for catalase (Sw_P00432, 506 amino acids, pI 6.41, 57.6 kDa), 0.818 for subtilisin (Sw_P00780, residues 106–379, 274 amino acids, pI 6.57, 27.3 kDa), 1.25 for thaumatin (Sw_P02883, 207 amino acids, pI 8.46, 22.2 kDa), 1.97 for α-lactalbumin (Sw_P00711, residues 20–142, 123 amino acids, pI 4.80, 14.2 kDa), 1.06 for D-xylose isomerase (Sw_P24300, 387 amino acids, pI 5.00, 43.1 kDa), 1.54 for trypsin (Sw_P00760, residues 21–243, 223 amino acids, pI 8.69, 23.3 kDa), 1.42 for pepsin (Sw_P00791, residues 60–387, 327 amino acids, pI 3.42, 34.6 kDa) and 0.70 for ovalbumin (Sw_P01012, 385 amino acids, pI 5.19, 42.8 kDa). The concentration of xylanase was calculated by comparison to the original stock solution provided by Hampton Research. The concentration of azidometmyoglobin was measured using an A_{409} extinction coefficient of 171 mM^{-1} cm^{-1} (Sw_P68082, 153 amino acids, pI 7.36, 17 kDa). Final values are reported in Table 2.

2.4. Crystal screening and the preparation of an initial precipitant/precipitant–additive screen

Two crystallization screens were tested: the commercially available sparse-matrix Index Screen (Hampton Research) and the P/PA screen designed for this study. The crystal screens were set up at ambient temperature (295 $\pm$ 1 K) in 96-well three-drop Greiner trays (Hampton Research) using protein solutions at a concentration of one-half the saturation level. All the crystallization trays were prepared using a Cartesian dispensing system (Model 96C-550-4S, Genomic Solutions, Irvine, CA, USA), a Honeybee sitting-drop crystallization robot (Genomic Solutions, Irvine, CA, USA) and an RS-3000 plate sealer (Brandel, Gaithersburg, MD, USA). Two samples of each protein, one in a standard buffer and one in optimized buffer solutions, were tested in the same tray against the same well solution. The Cartesian robot was used to place 100 µl of each crystal condition from a 96-well deep-block storage tray to the reservoir of the Greiner plate. The Honeybee robot was then used to dispense the crystallization drops in the tray (1 µl drops = 0.5 µl well solution + 0.5 µl protein solution). The trays were then stored at room temperature.

A new two-step crystal screen, P/PA, was developed for this study. Three components, salt, buffer and precipitating agents, comprise the majority of sparse-matrix crystal screening conditions. For the two-step experiments, the buffer and salt conditions were defined by the solubility screen and crystallization experiments were used to define the precipitating agent and possible additives. The P/PA screen is composed of 96 different conditions for use in a standard 12 $\times$ 8 96-well format. The 96-well screen is divided into three major sections, each containing 32 conditions. The identity of reagents and concentrations are given (Table 3). The first section screens three types of precipitating agents: polyethylene glycols, high-concentration salts including phosphates at various pHs and low-molecular-weight alcohols. The second section (32 conditions) is a set of additives in 20%(*w*/*v*) PEG 4000 and the third section is the same additive set in 30%(*v*/*v*) MPD. The additives used include polyamines, polyacids, sugars, zwitterions, multivalent metal ions, reducing agents, organic compounds, detergents, cofactors and cryoprotectants which are not normally found in the initial crystal screens (Table 3). The deep-well storage block was set up using eight columns and 12 rows, with consecutive numbered wells in columns beginning in the upper left corner. The order of conditions is such that like compounds are localized in separate regions of the first sector.

Table 3
Precipitant/precipitant–additive screen conditions.

With the salt and buffer conditions defined by the solubility screen, a minimal screen of precipitating agents and additives was prepared as listed and used in three-part 96-well multi-sitting-drop crystallization trays. The first 32 conditions are precipitating agents only including PEGs, alcohols and high-salt conditions. The second 32 conditions are a set of additives all in 20%(*w*/*v*) PEG 4000 and the last 32 condition are a repeat of the additives in 30%(*v*/*v*) 2-methyl-2,4-pentanediol (MPD).

(*a*) Precipitant screen.

No.	Content
1	20%(*w*/*v*) PEG 400
2	40%(*w*/*v*) PEG 400
3	20%(*w*/*v*) PEG 1000
4	40%(*w*/*v*) PEG 1000
5	1 *M* ammonium sulfate
6	2 *M* ammonium sulfate
7	10% ethanol
8	20% ethanol
9	10%(*w*/*v*) PEG 4000
10	20%(*w*/*v*) PEG 4000
11	10%(*w*/*v*) PEG 6000
12	20%(*w*/*v*) PEG 6000
13	1 *M* $(NH_4)_2HPO_4$
14	2 *M* $(NH_4)_2HPO_4$
15	10% 2-propanol
16	20% 2-propanol
17	10%(*w*/*v*) PEG 8000
18	20%(*w*/*v*) PEG 8000
19	10%(*w*/*v*) PEG 20000
20	20%(*w*/*v*) PEG 20000
21	1 *M* Na,K tartrate
22	2 *M* Na,K tartrate
23	15% ethylene glycol
24	30% ethylene glycol
25	2 *M* Na,K phosphate pH 5.8
26	2 *M* Na,K phosphate pH 5.8
27	2 *M* Na,K phosphate pH 5.8
28	2 *M* Na,K phosphate pH 5.8
29	1 *M* lithium sulfate
30	2 *M* lithium sulfate
31	15%(*v*/*v*) 2-MPD
32	30%(*v*/*v*) 2-MPD

Table 3 (continued)

(*b*) Precipitant–additive screen. Nos. 33–64, 20%(*w*/*v*) PEG 4000; Nos. 65–96, 30%(*v*/*v*) MPD.

Nos.	Content
33, 65	25 m*M* spermine
34, 66	25 m*M* spermidine
35, 67	25 m*M* imidazole
36, 68	25 m*M* urea
37, 69	25 m*M* guanidine–HCl
38, 70	25 m*M* L-arginine
39, 71	10%(*v*/*v*) triethylamine
40, 72	25 m*M* sodium thiosulfate
41, 73	25 m*M* sodium malonate
42, 74	25 m*M* sodium oxalate
43, 75	25 m*M* sodium citrate
44, 76	25 m*M* taurine
45, 77	10%(*w*/*v*) D-glucose
46, 78	10%(*w*/*v*) D-sucrose
47, 79	10%(*w*/*v*) dextrose
48, 80	10%(*w*/*v*) xylitol
49, 81	25 m*M* glycine
50, 82	25 m*M* D-alanine
51, 83	25 m*M* γ-aminobutyric acid
52, 84	25 m*M* ε-aminocaproic acid
53, 85	25 m*M* sodium thiocyanate
54, 86	2 m*M* octyl-β-glucoside
55, 87	2 m*M* ATP
56, 88	10%(*v*/*v*) glycerol
57, 89	10 m*M* calcium chloride
58, 90	10 m*M* zinc chloride
59, 91	10 m*M* potassium fluoride
60, 92	10 m*M* sodium iodide
61, 93	2 m*M* DTT
62, 94	2 m*M* TCEP–HCl
63, 95	10%(*v*/*v*) dioxane
64, 96	10%(*v*/*v*) dimethylsulfoxide

2.5. Crystal scoring

The results were recorded after one week at ambient temperature (295 ± 1 K). A Rhombix digital imager (Data-Centric Automation, Nashville, TN, USA) was used to image the drops. Images were taken with bright field and with polarized light exposure to ensure proper interpretation. The drops were scored by visual inspection of JPEG images in two categories: negative results of clear drops, precipitate and phase separation, and size-based positive results of crystalline precipitate, microcrystals, small crystals (<0.1 mm on longest edge), which all require additional optimization, and large crystals (>0.1 mm on longest edge).

3. Results

3.1. Solubility screening for protein solubility optimization

Comparison of relative solubility in various salts and buffers was completed by recovering protein from precipitation. Proteins were precipitated by the addition of PEG 8000 to a final concentration of 20%(*w*/*v*) and salts and buffers were added to aliquoted samples to test their effect on concentration of soluble protein. Supernatants were measured for soluble protein and then compared with the sample precipitated in water only as a control (Table 1). An optimized solution was then chosen for each protein by selecting a buffer and a salt if solubility was enhanced over that of water alone. Two new samples of each protein were prepared; one in optimized solution and one in a standard solution of 100 m*M* NaCl and 50 m*M* Tris–HCl pH 7.5. Saturation was obtained using centrifugal concentrators until a precipitate appeared and concentrations of protein in the filtered supernatant were then determined using UV absorbance and calculated conversion factors (Table 2). While not a measure of solubility of the protein in a supersaturated state where crystals nucleate and grow, this value is a simple measure of the relative effect of pH and salt on protein solubility which are readily accessible for a previously uncrystallized protein. Five proteins had a substantial increase in the saturation level when standard and optimal buffers were compared (Table 2, proteins 1–5). Two proteins displayed slight increases in solubility (Table 2, proteins 6 and 7) while three proteins had slight to modest decreases in solubility (Table 2, proteins 8–10).

The optimal solutions were determined from the solubility screen results (Table 1) and are summarized in Table 2. For catalase, decreases in solubility were noted for all the chloride

Table 4
Index and P/PA screen results.

Ten test proteins were subjected to two 96-condition crystallization screens: the Index screen (Hampton Research) and the P/PA screen described here. For each protein, two solutions were prepared, one in a standard buffer (Std) and a second in a customized optimal buffer (Opt) based on results from the solubility screen. A multidrop crystal tray was used and two drops, one from each buffer condition, were placed to equilibrate against the same well. Results were tabulated by visualization and a subjective process of classifying the equilibrated drops as clear (C), precipitate (ppt) and phase separation (phase) for negative results and microcrystalline material (μx) and large crystals (lgx) for positive results (in bold). Presented are the total numbers for each category. Numbers in parenthesis indicate results in the precipitant-only section of the P/PA screen.

	Index Screen					P/PA screen				
	C	ppt	phase	μx	lgx	C	ppt	phase	μx	lgx
Catalase										
Std	55	2	9	**9**	**21**	60	2	17	**14 (0)**	**3 (0)**
Opt	32	53	10	**0**	**1**	49	4	13	**19 (1)**	**0**
Subtilisin										
Std	85	3	8	**0**	**0**	90	0	5	**1 (0)**	**0**
Opt	68	9	18	**1**	**0**	76	7	8	**5 (2)**	**0**
Thaumatin										
Std	92	0	3	**0**	**1**	96	0	0	**0**	**0**
Opt	74	7	2	**2**	**11**	92	1	0	**2 (2)**	**1 (1)**
Xylanase										
Std	29	3	1	**62**	**1**	63	17	11	**5 (5)**	**0**
Opt	62	4	9	**8**	**13**	74	8	4	**7 (5)**	**3 (1)**
α-Lactalbumin										
Std	86	4	4	**1**	**1**	87	3	5	**1 (0)**	**0**
Opt	81	3	7	**3**	**2**	84	2	6	**3 (3)**	**1 (1)**
D-Xylose isomerase										
Std	56	13	4	**7**	**16**	12	30	41	**11 (5)**	**2 (0)**
Opt	42	10	4	**13**	**27**	76	4	4	**7 (6)**	**5 (3)**
Trypsin										
Std	58	16	22	**0**	**0**	94	1	0	**1 (1)**	**0**
Opt	65	14	9	**8**	**0**	93	1	0	**2 (1)**	**0**
Pepsin										
Std	83	4	6	**3**	**0**	86	1	7	**2 (2)**	**0**
Opt	64	14	4	**14**	**0**	81	5	6	**4 (4)**	**0**
Ovalbumin										
Std	59	7	29	**1**	**0**	72	13	11	**0**	**0**
Opt	53	4	36	**2**	**1**	33	34	28	**1 (1)**	**0**
Myoglobin										
Std	65	11	16	**4**	**0**	45	17	29	**5 (2)**	**0**
Opt	69	3	17	**7**	**0**	34	22	36	**4 (1)**	**0**

salts and the majority of the sodium salts. An increase in solubility was noted for disodium phosphate and dramatic increases were noted for trisodium citrate and sodium *N*-tris(hydroxymethyl)methyl-3-aminopropanesulphonate (Na TAPS) pH 8.5 buffer. Based on these results, an optimized solution of 50 m*M* Na TAPS pH 8.5 and 100 m*M* trisodium citrate was formulated. Subtilisin displayed high solubility in pure water. The salts added had marginal effects, but a slight increase was noted for Na TAPS pH 8.5 buffer and for calcium chloride. The optimized solution for subtilisin of 10 m*M* $CaCl_2$ and 50 m*M* Na TAPS pH 8.5 buffer was chosen. Calcium chloride was introduced at the concentration of an additive, where 10 m*M* instead of 100 m*M* was used in the hope of minimizing false positives in the crystal screens. Thaumatin and xylanase displayed high solubility in water. For thaumatin, 50 m*M* Na PIPES pH 6.5, which showed the least decrease in solubility, was used as the optimized solution. A composite solution of 100 m*M* sodium formate and 50 m*M* Na TAPS pH 8.5 buffer was chosen for xylanase. Salts appear to be necessary for α-lactalbumin and D-xylose isomerase solubility. Like catalase, an optimized solution of 50 m*M* Na TAPS pH 8.5 and 100 m*M* trisodium citrate was chosen for α-lactalbumin. Two components, 100 m*M* sodium cacodylate pH 7.0 and 50 m*M* Na TAPS pH 8.5, comprise the optimal buffer chosen for D-xylose isomerase. For trypsin, addition of salt reduced solubility. The buffer 50 m*M* Na TAPS pH 8.5 resulted in the smallest drop in solubility compared with water and was chosen as the optimized solution. Pepsin and azido-metmyoglobin displayed poor recovery from precipitation, with the exception of 50 m*M* Na TAPS pH 8.5, which was chosen for both proteins. Ovalbumin is very soluble in water alone and the chloride salts appear to decrease solubility significantly. An optimized solution of 50 m*M* Na HEPES pH 7.5 was used for this protein.

3.2. Comparison of crystal screen results for standard and solubility optimized protein solutions

The proteins were subjected to two crystal screens: the commercially available Index Screen (Hampton Research) and the P/PA screen described here. Crystal trials were set up with protein concentrations at approximately 1/2 of their saturation level (Table 2). The initial drop concentration was 1/4 maximal solubility after mixing with well solution. The results for all crystal trials are summarized in Table 4. The ten proteins displayed a variety of differences between the presence of standard buffer solutions and optimized solutions. Formation of microcrystals or large crystals are termed positive results and clear solutions, precipitate formation or phase separation are termed as negative results in the discussion that follows.

Overall, a total of 349 positive hits were observed for the ten proteins, evenly divided between protein in standard buffer with 172 hits and protein in optimized buffer with 177 positive hits. A significant difference is noted for conditions which produced large crystals: 45 conditions for five proteins in standard buffer and 65 conditions for six proteins in optimized buffer. Within the category of large crystals, the optimized conditions produced substantially larger more uniform crystals. It was clear in all cases that the large crystals seen for protein in the standard buffer needed significantly more optimization. The optimized buffer also decreased the number of microcrystalline results and increased the percentage of hits which were classified as large crystals. For protein in standard buffer, 127 of 172 (74%) positive conditions produced microcrystals. In comparison, protein in optimized buffer yielded 112 of 177 (63%) positive conditions that produced microcrystals. These results are not simply a shift in the distribution towards larger crystals. Instead, we find that positive hits are more evenly distributed over the ten proteins in optimal buffer. The positive hits for standard buffer appear primarily for just a few proteins. An example of this can be found in the results for xylanase. Xylanase in standard buffer produced positive hits in 68 (35%) of the conditions tested (192) and 67 of the 68 conditions produced microcrystals. By

comparison, protein in optimized buffer produced fewer positive hits (31) but substantially more (16) in the large crystal category.

Catalase had the most pronounced increase in solubility from 11 mg ml^{-1} in standard buffer to 40 mg ml^{-1} in optimized buffer (Table 2), but the optimal buffer displayed a negative effect in the crystal trials. The screens in standard buffer and optimal buffer were set up at 6 and 20 mg ml^{-1}, respectively. More than half (60%) of the drops in standard buffer remained clear, while only 42% of the drops in optimized buffer, with the greater amount of protein, were clear upon equilibration. With the Index Screen, optimal buffer yielded far fewer crystal conditions (30 *versus* one); however, with the P/PA screen the optimal and standard solutions yielded an approximately equal number of crystal conditions (19 *versus* 17, respectively). The small needles observed in standard buffer did not appear anywhere with optimized buffer (Fig. 1*a*). To determine whether an excess of protein caused the absence of large crystals in the optimized buffer trials, a second set of catalase crystal screens set up at 10 mg ml^{-1} protein stock (1/4 the saturation level concentration) in optimal buffer was attempted, but similar results were again obtained. This is the only protein tested where standard buffer produced a greater number of conditions producing large crystals (24) compared with the optimal buffer (one). A greater percentage of optimal buffer screens resulted in phase separation or precipitate formation (42%) than the standard buffer (16%). It may be that the energetic barrier to aggregate formation was lowered (by increasing solubility) to near-zero values, favoring precipitate over crystal formation.

Subtilisin, thaumatin and xylanase all show significant improvements in solubility (Table 2). Subtilisin, which displayed a threefold increase in solubility, had very few positive hits. The vast majority of positive results (six of the seven total) were seen in optimal buffer, with six optimal buffer conditions producing well formed microcrystals, whereas the only positive standard buffer condition produced a microcrystalline precipitate. The differences for thaumatin were even more significant. The crystal screens produced only one positive result with standard buffer, whereas the optimal buffer produced 16 positive hits with 12 conditions in the large crystal category. Two of the best crystals in optimized buffer were grown in sodium/potassium tartrate as previously reported for thaumatin (PDB code 1qrw; Index No. 31 and P/PA No. 21; Fig. 1*b*). Large single crystals also grew from optimal buffer in other high-salt conditions, including 1.8 *M* ammonium citrate (Index No. 21) and 30% Jeffamine (Index No. 38), where the drops with standard buffer remained clear (Fig. 2). In the xylanase crystal screens, the optimal buffer produced fewer overall positive conditions but a rather dramatic improvement in crystal quality was noted. The standard buffer results had a total of 68 positive hits and the optimal buffer had only 31 positive hits. However, all positive results in standard buffer where microcrystalline precipitate with a few producing small microcrystals. In contrast, the optimal buffer produced large single crystals in 16 of the 31 positive conditions (Fig. 1*c*).

The proteins α-lactalbumin and D-xylose isomerase show a slight increase in solubility (Table 2) and modest improvements in the total positive crystal hits (Table 4). The number of positive hits increased from three to

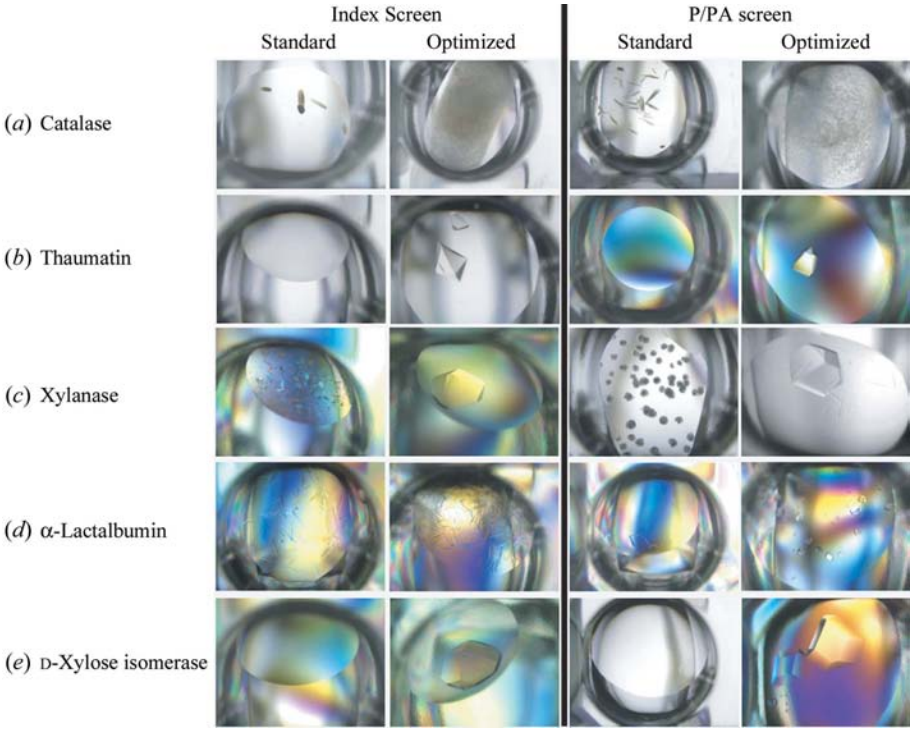

Figure 1
Crystal screen results of proteins in standard and optimized buffers in two crystal screens: Index (Hampton Research) and P/PA (Table 3). Images were obtained using a Rhombix automated imager using either bright field or polarized light. The wells are presented in pairs: the left image is of standard buffer and the right image is of optimized buffer. (*a*) Two examples of catalase are shown. The left pair is Index No. 91 and the right pair is P/PA No. 39. Here, the optimal buffer showed only precipitate. (*b*) Examples of thaumatin crystals grown from sodium/potassium tartrate are shown. The left pair is from Index No. 31 and the right pair is from P/PA No. 21. Large single crystals grew in optimized buffer and only a light oily precipitate formed in the standard buffer. (*c*) Positive results for xylanase are presented for both standard and optimal buffer. The visual quality of the crystals was far superior in the optimal buffer. The left pair is Index No. 75 and the right pair is P/PA No. 27. (*d*) The α-lactalbumin crystals showed comparable results in both standard and optimized buffer. The left pair is Index No. 2 and the right pair is P/PA No. 6. A modest improvement in solubility between buffers for α-lactalbumin did not translate into a dramatic improvement in crystal quality. (*e*) Examples of D-xylose isomerase crystals where large single crystals grew in optimized buffer with oily precipitate present in the standard buffer for many conditions. The left pair is Index No. 94 and the right pair is P/PA No. 65.

nine and from 36 to 52 for α-lactalbumin and D-xylose isomerase, respectively. For α-lactalbumin, both standard and optimal buffers produced large crystals in the same conditions (Fig. 1*d*). A very significant increase in number of conditions producing large crystals of D-xylose isomerase was noted, from 18 in standard buffer to 32 positive hits in optimized buffer (Fig. 1*e*). In the case of ovalbumin, only the optimal buffer resulted in the production of large crystals in one condition. No large crystals were found for the last three proteins tested, which had limited or detrimental solubility results. In spite of the lack of improvement in solubility, the number of positive results did increase from one to 10 for trypsin, from five to 18 for pepsin, from one to four for ovalbumin and from nine to 11 for myoglobin.

3.3. Comparison of a commercial sparse-matrix screen with the two-step optimization screening strategy: uncoupling crystal screen components

The Index Screen and the P/PA screen, set up with the same proteins in standard and optimal buffers, provided a direct comparison of the two strategies. The Index Screen is a commercially available sparse-matrix screen. The P/PA screen described here is a systematic screen where two components, the salt and buffer, are defined separately in an initial solubility screen. The P/PA screen contains a precipitant-only section and two additive screen sections each with different precipitating agents. A total of 240 positive hits were noted for the Index Screen, with 113 (47%) in optimal buffer and 178 (74%) from three proteins: catalase, xylanase and D-xylose isomerase. In comparison, a total of 109 positive hits were noted in the P/PA screen, with 64 (59%) in optimal buffer and 76 (70%) from the three proteins mentioned above. As mentioned previously, the crystal quality improved with optimal buffer. In the Index Screen, 40 conditions grew crystals larger than 0.05 mm for five proteins in standard buffer. This number increased to 55 for six proteins in optimal buffer.

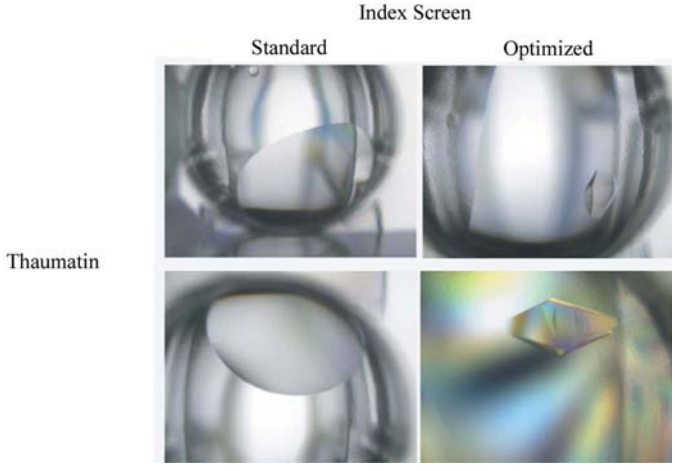

Figure 2
Large crystals of thaumatin grew in optimal buffer only. The top pair is 1.8 *M* triammonium citrate (Index No. 21) and the bottom pair is 30% Jeffamine (Index No. 38).

The P/PA screen contained fewer conditions (15) that produced large crystals, with five from two proteins in standard buffer and ten from four proteins in optimal buffer.

Overall, the Index Screen had a total of 95 of the 240 (40%) positive hits classified as large crystals, with 55 of the 95 (58%) from the optimal buffer. In comparison, the P/PA screen had 15 of the 109 (14%) classified as large crystals, with ten of the 15 (67%) from optimal buffer. The overall assessment clearly indicates that the sparse-matrix screen is substantially better than the systematic screen. It also indicates that optimized buffer improves crystal size in both screens. For the individual proteins, the Index Screen produced substantially more positive hits for six of the proteins when compared with the P/PA screen: 14 to three for thaumatin, 84 to 15 for xylanase, 63 to 25 for D-xylose isomerase, eight to three for trypsin, 17 to six for pepsin and four to one for ovalbumin. For a few proteins the numbers were approximately the same; seven to five for α-lactalbumin and 11 to nine for myoglobin. For catalase, the numbers for the P/PA screen showed an improvement, with 31 hits for Index and 36 hits for P/PA. Subtilisin showed the most improvement, with one positive hit for the Index screen and six positive hits for the P/PA screen.

The direct comparison of the two screens indicates that the sparse-matrix screen produced substantially more crystal conditions than the systematic screen. However, for all proteins, both screens produced positive results. The P/PA screen was developed to include additives in the initial screen. The proteins chosen for this study were not expected to be responsive to additives. We anticipated that the majority of positive results would occur in the precipitant-only section unless, of course, the protein crystallized in the precipitant chosen for the additive section. For the 109 total positive hits in the P/PA screen, 42 (39%) conditions were from the precipitant-only section. This total number includes a peculiar result for catalase in which 36 conditions produced crystals with only one from the precipitant-only section. For the remaining nine proteins, the precipitant-only section produced 41 of 73 (56%) of the positive results. The ability to produce crystals from a two-step process indicates that it is possible to uncouple the crystallization conditions.

4. Discussion

The solubility screen is a fast and simple method to determine some of the chemical parameters associated with crystallizing proteins. A twofold to threefold improvement in solubility was noted for half of the test proteins in this study when comparing a standard buffer against an optimized buffer as determined by the solubility screen. Solubility is measured by fractionating the protein between precipitated and dissolved states while measuring the effect of a select set of salts and buffers on the partitioning. The salts used are sets with common counterions. This allows a mix-and-match approach to deciding the best conditions for solubility. We have previously reported the use of the solubility screen to obtain crystals of an archaeal endonuclease (Collins *et al.*, 2004). In that study, the protein was dialyzed against deionized water to invoke precipitation.

Here, we report the use of PEG 8000 as a precipitating agent to drive the protein from solution. Salts and buffers are then added to recover the protein from precipitate. This was necessary since the ten test proteins were all moderately soluble in water. A third method can be used where salts and buffers are added to aliquots of protein prior to precipitation by PEG 8000. This last method may prove to be most valuable with proteins that cannot tolerate any type of precipitation.

It is our hypothesis that stabilization of the protein in the solution state moderates protein–protein interactions favoring nucleation and crystal growth. Enhancing solubility creates the condition where competing pathways to amorphous precipitation are minimized. The solubility screen presented here investigates a small fraction of the possible chemical components, but it is very simple to customize this type of screen to include as many components as desired. One might also consider repeating the screen at different temperatures. It has been noted in our laboratory that proteins crystallize at the temperature at which they are most soluble. If the goal were to subject the protein to a battery of sparse-matrix screens, then perhaps choosing the appropriate temperature beforehand would eliminate a large number of unnecessary trials.

The three-component sparse-matrix screens are classified as salts, buffers and precipitating agents. When a protein is introduced into the screen, two or more additional chemical parameters are introduced: the salt and buffer used in the protein solution. The buffer and salt components in the protein solution, which are constant, make standard crystal screens have five (or more) components. This may be a serious problem if one of the constant components is detrimental to crystal formation. This may be a factor for catalase, where the optimal buffer resulted in fewer positive results than standard buffer. The P/PA screen was less effective overall than the sparse-matrix screen, with only 109 positive hits compared with the 240 found with the sparse-matrix Index Screen. However, one should keep in mind that the P/PA screen is a single-component systematic screen where the buffer and salt are defined by a solubility screen. Additives are typically used in a second step when refining known crystallization conditions. Here, two-thirds of the P/PA screen conditions are intended to investigate various additives during the initial crystal screen. The proteins used in this study do not necessarily require specific additives for crystallization. However, the presence of additives in the first stage of crystal screening is potentially very advantageous for many of the new proteins being investigated by structural biologists.

The effect of improved solubility was tested in two crystal screens, the sparse-matrix Index Screen and the P/PA screen described here. Both screens provided quality results for proteins which showed improvement in solubility. Neither screen worked well for proteins that showed negligible improvement. In the case of catalase, which showed the greatest solubility enhancement in optimal buffer, solubility may have increased to a point where precipitate formation was favored for thermodynamic reasons. For several proteins, the optimized buffers resulted in dramatic improvement in crystals grown in the small drops (0.5 µl protein + 0.5 µl well solution) of the 96-well sitting-drop screens, with 65 screens producing large crystals for optimal buffer and 45 screens producing large crystals for standard buffer. In some cases, very large single crystals grew in optimal buffer where precipitate formed in the standard buffer (Fig. 1). The higher quality crystals grew from conditions where the amorphous precipitation is not present. Our assumption is that the higher solubility lowers the energetic barrier (surface tension) to crystal nucleation and produces moderate protein–protein interactions that create a greater potential for crystal nucleation and growth as opposed to precipitation of an amorphous state. Values of surface tension near zero result in precipitate formation. The lower surface tension allows nucleation and subsequent crystal growth at modest supersaturation, which is expected to lead to higher quality crystals. The large crystals grown in optimal buffer did visually appear more uniform than those grown in the standard buffer.

Improvements in the solubility screen are currently being investigated. These include the comparison of solubility results with dynamic light-scattering results and increasing sensitivity using non-specific fluorescent probes for detection of soluble protein. To further minimize the amount of protein, the adaptation of a submicrolitre crystallization robot to a small-scale solubility screen is being attempted.

The authors wish to thank Juliette Devos, Leif Hanson, Bob Cudney and Stephen Tomanicek for proofreading this manuscript and for helpful suggestions. This material is based upon work supported by the National Science Foundation under Grant No. 0346960 and The University of Toledo. Any opinions, findings and conclusions or recommendations expressed in this material are those of the authors and do not necessarily reflect the views of the National Science Foundation.

References

Bonneté, F. & Vivarès, D. (2002). *Acta Cryst.* D**58**, 1571–1575.
Brzozowski, A. M. & Walton, J. (2001). *J. Appl. Cryst.* **34**, 97–101.
Carter, C. W. Jr & Carter, C. W. (1979). *J. Biol. Chem.* **254**, 12219–12223.
Collins, B., Stevens, R. C. & Page, R. (2005). *Acta Cryst.* F**61**, 1035–1038.
Collins, B. K., Tomanicek, S. J., Lyamicheva, N., Kaiser, M. W. & Mueser, T. C. (2004). *Acta Cryst.* D**60**, 1674–1678.
Collins, K. D. (2004). *Methods*, **34**, 300–311.
Cudney, R., Patel, S., Weisgraber, K., Newhouse, Y. & McPherson, A. (1994). *Acta Cryst.* D**50**, 414–423.
Cumbaa, C. A., Lauricella, A., Fehrman, N., Veatch, C., Collins, R., Luft, J., DeTitta, G. & Jurisica, I. (2003). *Acta Cryst.* D**59**, 1619–1627.
D'Arcy, A. (1994). *Acta Cryst.* D**50**, 469–471.
DeLucas, L. J., Bray, T. L., Nagy, L., McCombs, D., Chernov, N., Hamrick, D., Cosenza, L., Belgovskiy, A., Stoops, B. & Chait, A. (2003). *J. Struct. Biol.* **142**, 188–206.
Durbin, S. D. & Feher, G. (1996). *Annu. Rev. Phys. Chem.* **47**, 171–204.
Gao, W., Li, S.-X. & Bi, R.-C. (2005). *Acta Cryst.* D**61**, 776–779.
Gasteiger, E., Gattiker, A., Hoogland, C., Ivanyi, I., Appel, R. D. & Bairoch, A. (2003). *Nucleic Acids Res.* **31**, 3784–3788.

Gilliland, G. L., Tung, M., Blakeslee, D. M. & Ladner, J. E. (1994). *Acta Cryst.* D**50**, 408–413.
Good, N. E., Winget, G. D., Winter, W., Connolly, T. N., Izawa, S. & Singh, R. M. M. (1966). *Biochemistry*, **5**, 467–477.
Jancarik, J. & Kim, S.-H. (1991). *J. Appl. Cryst.* **24**, 409–411.
Jancarik, J., Pufan, R., Hong, C., Kim, S.-H. & Kim, R. (2004). *Acta Cryst.* D**60**, 1670–1673.
Kulkarni, A. M. & Zukoski, C. F. (2002). *Langmuir*, **18**, 3090–3099.
McPherson, A. (1999). *Crystallization of Biological Macromolecules.* Cold Spring Harbor, New York: Cold Spring Harbor Laboratory Press.
McPherson, A. (2001). *Protein Sci.* **10**, 418–422.
Mueser, T. C., Rogers, P. H. & Arnone, A. (2000). *Biochemistry*, **39**, 15353–15364.
Page, R., Grzechnik, S. K., Canaves, J. M., Spraggon, G., Kreusch, A., Kuhn, P., Stevens, R. C. & Lesley, S. A. (2003). *Acta Cryst.* D**59**, 1028–1037.
Page, R. & Stevens, R. C. (2004). *Methods*, **34**, 373–389.
Rupp, B., Segelke, B. W., Krupka, H. I., Lekin, T., Schafer, J., Zemla, A., Toppani, D., Snell, G. & Earnest, T. (2002). *Acta Cryst.* D**58**, 1514–1518.
Stura, E. A., Satterthwait, A. C., Calvo, J. C., Kaslow, D. C. & Wilson, I. A. (1994). *Acta Cryst.* D**50**, 448–455.
Tardieu, A., Bonneté, F., Finet, S. & Vivarès, D. (2002). *Acta Cryst.* D**58**, 1549–1553.
Wooh, J. W., Kidd, R. D., Martin, J. L. & Kobe, B. (2003). *Acta Cryst.* D**59**, 769–772.